A DFT Study of the Interstitial Chemical Shifts in Main Group Element Centered Hexazirconium Halide Clusters

Jingyi Shen and Timothy Hughbanks*

Department of Chemistry, Texas A&M University, College Station, Texas, 77843-3012

Received: September 18, 2003; In Final Form: October 28, 2003

A density functional theoretical study aimed at correlating the chemical shifts of interstitial atoms and electronic structures of main-group-centered hexazirconium halide clusters has been performed and analyzed within the framework of perturbation theory. The influence of bridging halides on electronic structure was studied with two series of model compounds $[(Zr_6Z)X_{12}](H_2O)_6^{n+}$ (Z = B, C; X = Cl, Br, I). The effect of terminal ligands on electronic structure was investigated with model compounds $[(Zr_6B)Cl_{12}]L_6^+$ (L = H_2O, PH_3, HCN, and OPH_3). There is a qualitative inverse proportionality between the chemical shifts and the calculated energy gaps between two Kohn−Sham orbitals, $\Delta E(t_{1u}^* - t_{1u})$, where t_{1u} and t_{1u}^* orbitals are the bonding and antibonding orbitals that result from the interaction between the zirconium cage bonding orbitals and the interstitial 2p orbitals. Chemical shielding properties of the interstitial atoms were further calculated with the gauge-including atomic orbitals (GIAO) method.

Introduction

NMR spectroscopy has proven to be an invaluable analytical tool for characterizing centered hexanuclear zirconium halide clusters (Figure 1), $[(Zr_6ZX_{12})L_6]^{m-}$ (X = Cl, Br, I; Z = H, Be, B, C, N, Mn, and Co; L = various ligands), as species in solution[1−5] and as building blocks in the solid state.[1] NMR spectroscopy serves a more central and comprehensive analytical role in the study of $[(Zr_6ZX_{12})L_6]^{m-}$ based clusters than is possible for any other polynuclear metal clusters. This fact derives from a fortunate confluence of circumstances: The electronic environment immediately surrounding the interstitial (Z) atom has nearly octahedral symmetry and the electric field gradient at the nucleus is small enough that quadrupolar broadening of Z-nucleus resonances is dramatically curtailed. This is true even when the distribution of ligands (L) on the cluster exterior is quite asymmetric.[2] Fortunately, the interstitial nucleus is sensitive enough to the presence of ligands on the exterior of the cluster to be a useful probe of their presence via changes in chemical shift and, sometimes, spin−spin coupling. Therefore, within the class of Z-centered hexanuclear zirconium clusters, NMR spectroscopy has high resolution, good sensitivity, a chemical shift range with useful breadth and interpretive simplicity. These molecules also offer invaluable potential for studying trends in NMR properties since no other series of molecules offers such a variety of nuclei within a single chemical environment.

The most remarkable characteristic of chemical shifts exhibited by interstitial atoms in clusters is that they are quite generally outside the range exhibited by "ordinary" diamagnetic molecules. For carbide-, boride-, and nitride-centered carbonyl-ligated clusters of the later transition metals, such exceptional chemical shifts have also been observed and are quite comparable to data for hexazirconium clusters.[6−13]

A number of correlative schemes have been put forward in an attempt to understand the origin and trends governing the deshielding of interstitial atoms in metal clusters. For example, Mason has attributed the increased interstitial deshielding of several main-group-centered clusters to compression of the cluster cavity.[14] Using the Fenske−Hall computational method in combination with the Ramsey sum over states (SOS) approximation, Khattar and Fehlner performed molecular orbital analysis of the ^{11}B NMR chemical shifts of boride-centered transition metal carbonyl clusters.[15−18] They concluded that the occupied and unoccupied orbitals that result from the perturbation of the 2p atomic orbitals of the interstitial boron and the related orbitals from empty metal clusters make main contributions to paramagnetic shielding. Kaupp calculated ^{13}C chemical shift tensors for interstitial carbides of a series of transition metal carbonyl clusters using sum-over-states density functional perturbation theory (SOS-DFPT)[17] and concluded that the downfield interstitial chemical shifts are directly related to the paramagnetic contribution involving interstitial carbon−metal bonding. Even modest structural anisotropies in M_nC cages gave rise to significant anisotropy of the chemical shift tensors. He further concluded that with other conditions being equal, expansion of the cluster core decreases the band gap and thus increases the paramagnetic contribution, in contradiction with Mason's heuristic arguments.

Harris and Hughbanks presented a qualitative analysis of the interstitial chemical shifts of centered hexazirconium halide

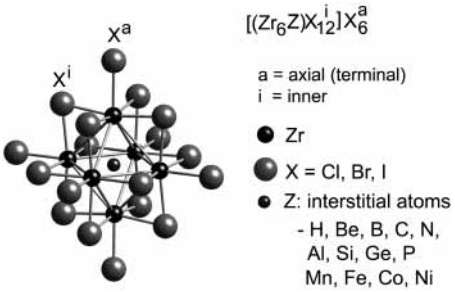

Figure 1. Schematic representation of centered hexazirconium clusters $[(Zr_6ZX_{12})X_6]^{m-}$.

* Corresponding author. E-mail: trh@mail.chem.tamu.edu. Tel: (979)-845-0215. Fax: (979)847-8860.

10.1021/jp0368029 CCC: $27.50
Published on Web 12/05/2003

clusters that focused on the paramagnetic term (σ_p) in Ramsey's chemical shift expression.[1] In the past few years, the rapid development of interpretive tools within density functional theory (DFT) has made it possible for efficient and accurate treatment of large systems such as transition metal clusters.[19−22] DFT in combination with the gauge including atomic orbitals method (DFT/GIAO) has evolved into an established method for computing chemical shielding properties.[23−32] In this paper we present work that extends the analyses of Harris and Hughbanks. We aim to establish more quantitative correlations between the interstitial chemical shifts and the electronic structures of boron- and carbon-centered zirconium halide clusters. (Similar studies, including those of transition-metal-centered clusters, could be performed if sufficient experimental data were available.)

To study the effect of bridging halide and terminal ligands on the interstitial ^{11}B and ^{13}C chemical shifts, a number of hypothetical compounds have been constructed that are closely related to structures of existing analogues. DFT single point energy calculations were carried out for model compounds and correlation between interstitial chemical shifts and energy gaps of selected Kohn−Sham orbitals was studied. Chemical shielding properties of interstitial atoms were further quantitatively evaluated with the DFT/GIAO method. No attempt to account for measured chemical shift variations due to solvation differences was made, though experimental studies indicate that such differences may account for chemical shift differences up to 2 ppm.[1,2,33−35]

Computational Details

All calculations of single-point energy and NMR properties for discrete model compounds were performed using density functional theory (DFT) in the Amsterdam density functional package (ADF).[36−38] The Becke exchange functional and the Lee−Yang−Parr correlation functional (BLYP) were utilized in the calculation.[39,40] Nuclear magnetic shielding tensors were calculated using the gauge including atomic orbitals (GIAO) method.[25,41,42] Two programs, namely, the stand-alone NMR program within the ADF program and the stand-alone EPR/NMR program, have been used for the calculation of chemical shielding tensors. When calculations use the same functional, same basis sets, and same SCF parameters, the two programs give comparable results. Both nonrelativistic calculations and relativistic calculations with the scalar zero-order-regular-approximation (ZORA) method were performed. Nonrelativistic calculations were performed with the stand-alone EPR/NMR program for detailed orbital contribution analysis. The scalar ZORA NMR calculations were performed with the stand-alone NMR program within the ADF program. For nonrelativistic calculations, the effect of basis sets on the chemical shielding properties was tested on $[(Zr_6BCl_{12})(H_2O)_6]^+$. On the basis of these tests, we chose to use the triple-ζ, double-polarization (TZ2P) basis functions for the interstitial atoms and the triple-ζ, single-polarization (TZP) basis functions for all other atoms. For the scalar ZORA calculations, we have performed tests with several more expanded basis functions, including the TZ2P basis functions for zirconium and quadruple-ζ, quadruple-polarization basis functions (QZ4P) for boron. All-electron basis sets were used for hydrogen and the interstitial boron and carbon atoms. The cores (Zr, 1s−3d; Cl, P, 1s−2p; Br, 1s−3p; I, 1s−4p; C, N, O, 1s) were treated within the frozen core approximation. The Dirac utility was used to generate relativistic frozen core potentials for the scalar ZORA calculations. The integration parameter *accint* and the energy convergence criterion were set at 6 and 10^{-6} au, respectively. Symmetry was lifted in all calculations. [Note: Users of the ADF program using Symmetry option should be certain that the parameter A1FIT is set high enough (say, 10 Å) to avoid errors that this method can otherwise introduce.[43]]

Geometries used in calculations of discrete cluster model compounds were based on structures of related compounds determined by X-ray crystallography.[4,35,44−47] To simplify calculations, the ligands PEt_3, $NCCH_3$, and $OPPh_3$ were respectively replaced by PH_3, NCH, and OPH_3 in the model compounds. When necessary, experimental structures were slightly idealized so that $[(Zr_6Z)X_{12}]$ cores exhibited O_h symmetry and in model compounds ligand rotational orientations were selected to achieve the highest possible symmetry. For the $[(Zr_6B)Cl_{12}]L_6^+$ series of compounds, both PH_3 and NCH ligated clusters adopt the same $[(Zr_6B)Cl_{12}]$ core structure as that of a water-terminated cluster, while the $L = OPH_3$ molecule adopts a slightly larger core (Zr−B distance being 0.015 Å longer) determined from the experimental structure of $[(Zr_6B)Cl_{12}](OPPh_3)_6^+$.[45] This geometrical invariance with change of terminal ligands is reflected in both experimental and unpublished theoretical results.[2,35,45,46] When no direct experimental data were available, estimates were made based on similar compounds. For example, the Zr−O distance in $[(Zr_6C)Cl_{12}](H_2O)_6^{2+}$ was estimated by calculating the differences in Zr−O distances in the $[(Zr_6B)X_{12}](H_2O)_6^+$ (X = Cl, Br, I)[4,35,44] series and assuming the same differences apply to the series $[(Zr_6C)X_{12}](H_2O)_6^{2+}$ (distances in the bromide and iodide compounds are known).[4,35,45] Detailed geometry information can be found in the Supporting Information.

Geometries of the ^{11}B-reference and ^{13}C-reference molecules (BCl_3 and TMS) were both optimized at the DFT/BLYP level with TZ2P all electron basis sets. The optimized (exptl.) boron−chlorine bond length was 1.730 (1.75 ± 0.02[48] by X-ray diffraction, 1.73 ± 0.02[49] by electron diffraction) Å, carbon−silicon bond length was 1.865 Å (1.93 ± 0.03 Å,[50] 1.89 ± 0.02 Å,[51] both by electron diffraction), and carbon−hydrogen bond was 1.103 Å (1.10 ± 0.05 Å[51] by electron diffraction). Chemical shielding properties of the references were calculated with the same theoretical method (DFT/BLYP/GIAO) as for the cluster compounds. To maintain consistency with the cluster compounds, TZ2P all-electron basis sets were used for the interstitial ^{11}B and ^{13}C atoms while TZP basis sets with small frozen cores were used for other atoms.

The electronic structure of the solid-state compound $Zr_6I_{12}C$ was also studied by use of density functional theory with the BLYP functional.[52] This is a cross-linked cluster compound with weak intercluster bonding, and a single *k* point ($k = 0$) energy calculation was performed using the DMol^3 program[53,54] in the Cerius2 v4.2 suite of programs. P1 symmetry was used in the calculation (the structure is $R\bar{3}$). The double numerical basis functions including d- and p-polarization functions (DNP) were employed in the calculation. Effective core potentials with frozen cores (1s2s2p3s3p3d) and (1s2s2p3s3p3d4s4p4d) were used for Zr and I, respectively. The energy convergence criterion was set at 10^{-6} au.

Results

Energy Gap between t_{1u} and t_{1u}* Orbitals. As discussed by Khattar and Fehlner, and illustrated by Harris and Hughbanks, qualitative understanding of the interstitial atom chemical shifts starts from Ramsey's formula from perturbation

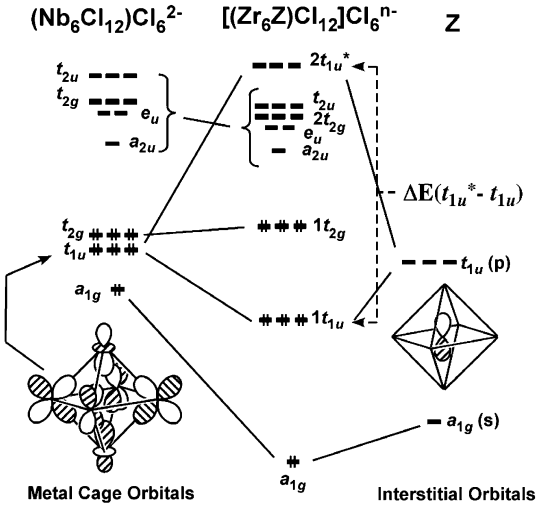

Figure 2. Schematic representation of molecular orbital diagram of main group element centered hexazirconium chloride clusters. The interaction between zirconium cage orbitals and interstitial p orbitals with t_{1u} manifold is highlighted.

theory (eqs 1−3) and focuses on the paramagnetic shielding.[1,15,18,55]

$$\sigma = \sigma_d + \sigma_p \tag{1}$$

$$\sigma_d(zz) = \frac{e^2}{2mc^2}\left\langle 0\left|\frac{x^2+y^2}{r^2}\right|0\right\rangle \tag{2}$$

$$\sigma_p(zz) = -\left(\frac{e\hbar}{2mc}\right)^2 \sum_n \left\{ \frac{\langle 0|L_z|n\rangle\left\langle n\left|\frac{2L_z}{r^3}\right|0\right\rangle}{E_n - E_0} + \frac{\left\langle 0\left|\frac{2L_z}{r^3}\right|n\right\rangle\langle n|L_z|0\rangle}{E_n - E_0} \right\} \tag{3}$$

The remaining components of the shift tensor are defined analogously. The paramagnetic shielding arises from the second-order mixing of paramagnetic excited states into the ground state in the presence of a perturbing magnetic field. The significant excitations must meet the following criteria simultaneously. First, the ground and excited states must have right symmetry to be coupled by the L operator. Since the clusters have rigorous or near O_h symmetry, this requirement means that the A_{1g} ground state will couple only to T_{1g} symmetry excited states. Second, the $1/r^3$ dependence more heavily weights terms, wherein the molecular orbitals of the ground and excited states both have significant contributions from the atomic orbitals on the interstitial atom. For the main-group-centered hexazirconium halide clusters, this means that the molecular orbitals involved must both have significant interstitial p contributions. Thus, molecular orbitals with t_{1u} symmetry make dominant contributions to the paramagnetic shielding. To summarize then, T_{1g} symmetry excited states created in excitations involving occupied t_{1u} and virtual t_{1u}* orbitals ($t_{1u}^5 t_{1u}$* configurations) should be important, and other excitations should be negligible. Finally, the magnitude of coupling is inversely proportional to the energy gap between the involved orbitals. The main contributions to paramagnetic shielding are expected to arise from excitations originating with one occupied set of t_{1u} orbitals involved in bonding the interstitial atom to the surrounding Zr_6 cage. In the simplest analysis, illustrated in Figure 2, the interstitial atom p orbitals mix with only one set of t_{1u} cage orbitals (a combination that would have Zr−Zr bonding character even in the absence of the interstitial atom), and a bonding−antibonding pair of t_{1u}-symmetry orbitals is generated. These two will be denoted as the t_{1u} and the t_{1u}* orbitals from this point forward. Since the energy gap between these two t_{1u} orbitals is the smallest of all the occupied virtual orbitals within the t_{1u} manifold, the matrix element involving these two orbitals should be the most significant among all contributions to the paramagnetic term. Hence, a correlation is anticipated between interstitial chemical shifts and the energy gaps between the t_{1u} and the t_{1u}* orbitals as the terminal and bridging ligands vary.

TABLE 1: Calculated Energy Gaps $\Delta E(t_{1u}^* - t_{1u})$ and Experimental ^{11}B or ^{13}C Chemical Shifts of Selected Boron- and Carbon-Centered Clusters

model compound		δ_{expt} (ppm)[a]	$\Delta E(t_{1u}^* - t_{1u})$ (eV)	solvent	ref.
		$[(Zr_6X_{12}B)L_6]^+$			
X =	L =				
I	H_2O	215.2 (H_2O)	3.670	H_2O	4
Br	H_2O	198.9 (H_2O)	3.999	H_2O	3
Cl	H_2O	189.9 (H_2O)	4.277	H_2O	3
Cl	PH_3	199.2 (PEt_3)	4.171	CH_2Cl_2	2
Cl	HCN	196.3 (MeCN)	3.843	MeCN	1,2
Cl	OPH_3	186.5 ($OPPh_3$)	4.519	CH_2Cl_2	45
		carbon centered clusters			
$[(Zr_6CCl_{12})(H_2O)_6]^{2+}$	464.6	5.153	est.[b]		4
$[(Zr_6CBr_{12})(H_2O)_6]^{2+}$	493.8	4.942	H_2O		4
$[(Zr_6CI_{12})(H_2O)_6]^{2+}$	531.6	4.518	H_2O		4
$Zr_6I_{12}C$	524.5[c]	4.773[d] (4.573[e])			45

[a] The real ligands are listed in parentheses. [b] Estimate was made by subtracting the chemical shift difference between $[(Zr_6CBr_{12})(CH_3OH)_6]^{2+}$ and $[(Zr_6CBr_{12})(H_2O)_6]^{2+}$ from the chemical shift of $[(Zr_6CCl_{12})(CH_3OH)_6]^{2+}$. [c] The ^{13}C chemical shift of $Zr_6I_{12}C$ was obtained from solid-state MAS measurement. [d] Energy gap was calculated with DMol^3 software. [e] Energy gap after correction for ADF-DMol^3 differences.

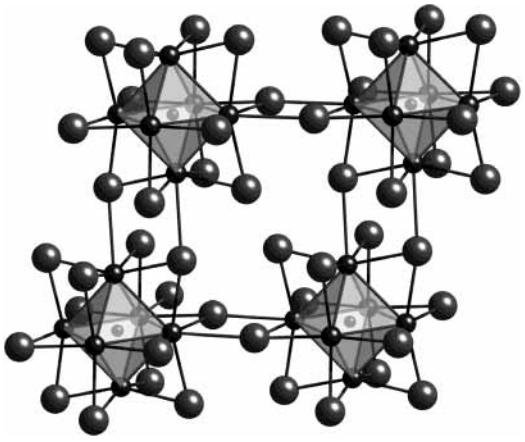

Figure 3. Intercluster linkage of cluster units in $Zr_6I_{12}C$.

The change of energy gap with bridging ligands was studied for both boron- and carbon-centered clusters using model compounds $[(Zr_6BX_{12})(H_2O)_6]^+$ and $[(Zr_6CX_{12})(H_2O)_6]^{2+}$ (X = Cl, Br, I). The change of energy gap with terminal ligands was studied using model compounds $[(Zr_6BCl_{12})L_6]^+$ (L = PH_3, NCH, H_2O, OPH_3). All energy gaps between the calculated t_{1u} and t_{1u}* Kohn−Sham orbitals were listed in Table 1.

Zr_6CI_{12}. Zr_6CI_{12} is a network solid consisting of cross-linked Zr_6CI_{12} clusters.[52] The coordination environments of the carbon atom and all metal atoms in the cluster are essentially the same as in the molecular clusters we have considered to this point, except that the ligands that cap the terminal positions on the metal atoms are iodides on neighboring clusters (see Figure 3). Zr−Zr distances between clusters (4.92 Å) are much longer than

TABLE 2: Calculated and Experimental Interstitial ^{11}B and ^{13}C Nuclear Shieldings of $[(Zr_6BX_{12})L_6]^+$ and $[(Zr_6CX_{12})(H_2O)_6]^{2+}$ at the Nonrelativistic Level

		ligand	σ_{iso} (ppm)	σ_p (ppm)	σ_d (ppm)	δ_{calcd}[a] (ppm)
			$[(Zr_6BX_{12})L_6]^+$			
X =	L =					
I	H_2O	−124.89	−361.58	236.69	215.19	215.2
Br	H_2O	−118.52	−334.87	216.35	208.82	198.9
Cl	H_2O	−110.74	−329.37	218.63	201.04	189.9
Cl	PH_3	−122.31	−340.91	218.61	212.61	199.2
Cl	HCN	−121.92	−338.34	216.41	212.22	196.3
Cl	OPH_3	−104.13	−330.09	225.96	194.43	186.5
			$[(Zr_6CX_{12})(H_2O)_6]^{2+}$			
X =	Cl	−335.99	−623.79	287.80	519.01	464.6
	Br	−351.86	−633.33	281.48	534.88	493.8
	I	−385.92	−688.27	302.35	568.94	531.6

[a] δ_{calcd} (^{11}B) = σ_{iso} (BCl_3) − σ_{iso} (Cluster) + δ_{ref} (BCl_3) = 42.604 − σ_{iso} (Cluster) + 47.7 δ_{calcd} (^{13}C) = σ_{iso} (TMS) − σ_{iso} (Cluster) + δ_{ref} (TMS) = 183.02 − σ_{iso} (Cluster) + 0.0. [b] The original source of the measurements are listed in Table 1.

within clusters (there are two unique Zr−Zr distances: 3.195(1) and 3.207(1) Å), and it is therefore reasonable to treat this as a quasi-molecular solid. In this case we can assume that periodic boundary conditions can be applied to the unit cell, which is virtually equivalent to the use of a single *k* point (k = 0) calculation. The inclusion of this compound in this study is of particular interest because it is a rare case of a centered hexazirconium cluster compound with 16 cluster bonding electrons (CBEs); the vast majority of known Zr_6ZX_{12} clusters have 14 CBEs.

The degeneracy of the t_{1u} orbitals is lifted to a small extent by the lowering of symmetry from O_h to S_6. The number of unoccupied orbitals with both zirconium 4d and carbon 2p contributions is much greater than that which was seen for the molecular compounds as a result of more extensive orbital mixing. These orbitals can be grouped into two sets of $\{2e_u + 2a_u\}$ orbitals, one about 5 eV and the other about 7 to 8 eV above the t_{1u} orbitals. The first set of orbitals is of special interest since the energy gap is comparable to the t_{1u}*− t_{1u} gap of the carbon-centered 14 CBE clusters. Since the $[(Zr_6C)]$ cage geometry is close to O_h we group the first $\{2e_u + 2a_u\}$ set into the "t_{1u} set" in order to relate the ^{13}C chemical shift of Zr_6CI_{12} with chemical shift trend of the $[(Zr_6CX_{12})(H_2O)_6]^{2+}$ series. A weighting method taking into consideration both the carbon 2p contribution and Kohn−Sham orbital energy has been used to calculate the energies of such hypothetical t_{1u}* orbitals. Details can be found in the Supporting Information. The energy gap $\Delta E(t_{1u}$*− $t_{1u})$ so derived is included in Table 1. Correction has also been made to account for a systematic 0.2 eV difference in the energy gap calculated using the DMol^3 and ADF programs.

Nonrelativistic Chemical Shielding Tensors. Nonrelativistic chemical shielding properties were calculated for each model compound. The total isotropic shielding (σ_{iso}) separates into diamagnetic and the paramagnetic terms (σ_d and σ_p, respectively) as defined within the GIAO formalism by Schreckenbach and Ziegler.[25,28] The isotropic components of the shielding tensors for boron- and carbon-centered clusters are summarized in Table 2. Detailed orbital contribution analyses to the paramagnetic term will be discussed later. The isotropic chemical shifts, δ_{calcd}, are calculated from the differences of isotropic shieldings (σ_{iso}): $\delta_{calcd} = \sigma_{ref} - \sigma_{iso} + \delta_{ref}$, where σ_{ref} refers to the isotropic shielding constant of the reference compound used for the theoretical calculation and δ_{ref} refers to the experimental chemical shift of the reference.[56] Both calculated and experimental chemical shifts for the model compounds are included in the corresponding tables. The calculations predict ^{11}B and ^{13}C isotropic chemical shifts are further downfield than we measure experimentally. The maximum relative errors for the calculated ^{11}B and ^{13}C isotropic chemical shifts are 8% and 12%, respectively. Correlations between the calculated ^{11}B and ^{13}C chemical shifts with the measured chemical shifts were shown in Figure 4 and Figure 5. It is clear that the calculated and measured chemical shifts are consistent.

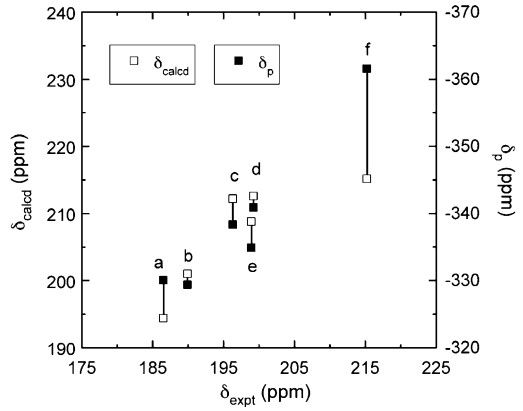

Figure 4. ^{11}B isotropic chemical shifts and paramagnetic shieldings vs measured chemical shifts (see Table 2). (a)−(d) are the $[(Zr_6BCl_{12})L_6]^+$ series. (a) L = OPH_3, (b) L = H_2O, (c) L = HCN, (d) L = PH_3, (e) $[(Zr_6BBr_{12})(H_2O)_6]^+$, (f) $[(Zr_6BI_{12})(H_2O)_6]^+$.

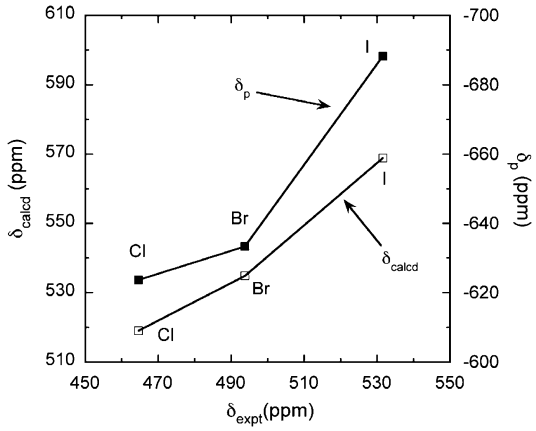

Figure 5. Correlation of calculated ^{13}C isotropic chemical shifts and paramagnetic shieldings with measured chemical shifts for $[(Zr_6CX_{12})(H_2O)_6]^{2+}$ (X = Cl, Br, I) (See Table 2).

Both the ^{11}B and ^{13}C shielding anisotropies in centered zirconium halide clusters are small in comparison with interstitial carbides in transition metal carbonyl clusters.[17] For cluster compounds with terminal ligands other than water, the calculated anisotropy is less than 1 ppm. For the water ligated clusters, the σ_{11} is slightly larger than σ_{22} and σ_{33} and is directed along the 3-fold axis. For the $[(Zr_6BX_{12})(H_2O)]^+$ series, the anisotropy increased from 11 to 18 ppm as the bridging halides progress from Cl to I. For the $[(Zr_6CX_{12})(H_2O)]^{2+}$ series, the anisotropy increased from 18 to 29 ppm.

Chemical Shielding Tensors: Nonrelativistic versus Scalar Relativistic ZORA. Our chemical shielding calculation at the nonrelativistic level successfully reproduced the ^{11}B chemical shift trend in the $[(Zr_6BX_{12})(H_2O)]^+$ (X = Cl, Br, I) series. The calculated chemical shift difference between the Cl- and Br-bridged clusters is well reproduced. Nevertheless, the calculated chemical shift difference between the Br- and I-bridged clusters is only 6 ppm, much less than the measured 16 ppm difference. Relativistic calculation at the scalar ZORA level was carried

TABLE 3: Comparison between ^{11}B Chemical Shifts of $[(Zr_6BX_{12})(H_2O)_6]^+$ Calculated at the Scalar ZORA and Nonrelativistic Levels

ligand (X=)	δ_{zora}[a] (ppm)	δ_{nonrel} (ppm)	δ_{expt} (ppm)
Cl	190.19	201.04	189.1
Br	196.14	208.82	198.9
I	202.23	215.19	215.2

[a] $\delta_{zora} = \sigma_{iso-zora}(BCl_3) - \sigma_{iso-zora}$ (Cluster) + δ_{ref} (BCl_3) = 42.201 − $\sigma_{iso-zora}$ (Cluster) + 47.7

out to investigate the possible influence of relativity. Chemical shifts calculated at both relativistic scalar ZORA and nonrelativistic levels are listed in Table 3 together with the experimental value. Both calculations utilized TZP/TZ2P basis functions as described in the computational details section. Chemical shifts for Cl- and Br-bridged clusters at relativistic ZORA levels are in better agreement with experiments. The chemical shift difference between the Br- and I-bridged clusters, however, was not improved by the inclusion of scalar relativistic effects. Relativistic scalar ZORA calculations with larger basis sets, i.e., TZ2P for Zr and QZ4P for B, were also performed. These larger basis-set computations did not improve results either, though we cannot be certain why that is so. It may be that spin−orbit coupling corrections are more important than those included in a scalar-only treatment. Investigations of organic systems have amply demonstrated that indirect "heavy-atom effects" on NMR chemical shifts of light-atom nuclei are primarily the result of spin−orbit induced mixing of nonzero spin states into diamagnetic ground states.[57] This could occur via Zr ($\zeta_{Zr(d)} \sim 400$ cm^{-1})[58] directly bound to the interstitial atoms or via two-bond coupling to the halides ($\zeta_{Br(p)} \sim 2500$ cm^{-1}, $\zeta_{I(p)} \sim 5100$ cm^{-1}).[59]

Discussion

Correlation between the Interstitial Chemical Shifts and the Energy Gap $\Delta E(t_{1u}^* - t_{1u})$. Interstitial atoms within hexazirconium halide clusters exhibit unusual downfield shifts compared with ordinary diamagnetic compounds. As we have indicated, this extreme downfield shift is mainly attributable to contributions from the paramagnetic term (σ_p). As discussed in the Results section, the most significant contribution to the paramagnetic contribution is proposed to come from the "excitation" between the t_{1u} and the t_{1u}^* orbitals as illustrated in Figure 2.

The plots presented in Figures 6 and 7 suggest a linear correlation between the interstitial chemical shifts and the inverse of calculated energy gap, $\Delta E(t_{1u}^* - t_{1u})$, for both boron- and carbon-centered clusters. This approximate inverse proportionality demonstrates that $t_{1u}^* - t_{1u}$ coupling in the paramagnetic term contributes most to the change in interstitial chemical shifts.

To find an exact linear correlation between the chemical shifts and $\Delta E^{-1}(t_{1u}^* - t_{1u})$, the following conditions would have to be satisfied simultaneously: (a) the diamagnetic term is constant; (b) contributions from other $t_{1u}-t_{1u}^*$ excitations are negligible, or at least constant; (c) the matrix elements coupling the t_{1u} and t_{1u}^* excitations must be invariant with changes of bridging halides and terminal ligands. Of course, these approximations are not entirely satisfied and an imperfect correlation is observed. Even though we assume the diamagnetic term varies on a smaller scale compared to the paramagnetic term, this variation will affect the correlation if the chemical shift range is not very broad, which is the case of boron-centered clusters. We expect an increase of the chemical shift range will reduce the relative

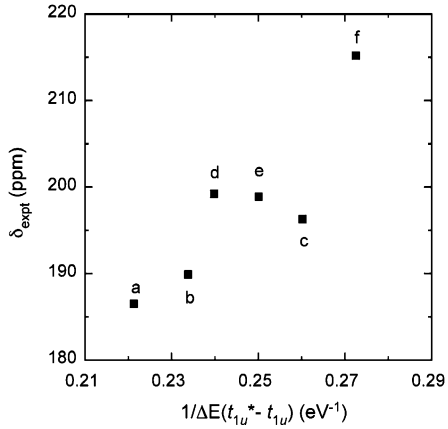

Figure 6. Correlation between measured ^{11}B isotropic chemical shifts and $\Delta E^{-1}(t_{1u}^* - t_{1u})$ for model compounds (see Table 1). (a)−(d) correspond to the $[(Zr_6BCl_{12})L_6]^+$ series. (a) L = OPH_3, (b) L = H_2O, (c) L = HCN, (d) L = PH_3, (e) $[(Zr_6BBr_{12})(H_2O)_6]^+$ (f) $[(Zr_6BI_{12})(H_2O)_6]^+$.

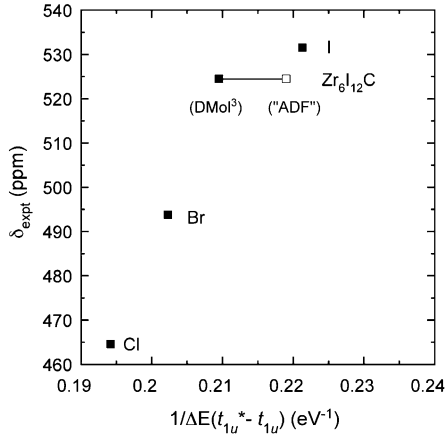

Figure 7. Correlation between measured ^{13}C chemical shifts and $\Delta E^{-1}(t_{1u}^* - t_{1u})$ for $[(Zr_6CX_{12})(H_2O)_6]^{2+}$ series and $Zr_6I_{12}C$ (see Table 1). (■) Direct calculation results. (□) ADF estimate derived from DMol^3 result and systematic energy gap difference between ADF and DMol^3 calculations.

effect of the diamagnetic term and enhance the linear correlation. This is supported by comparison of chemical shift range and correlation quality for boron- and carbon-centered clusters. Violation of the other two conditions could also contribute to imperfect linearity in the correlation, but it is difficult to predict to what extent they will affect the correlation.

As observed for boron- and carbon-centered hexazirconium halide clusters, the deshielding of the interstitial atoms increases as the bridging halides change from chlorine to iodine. For boron centered clusters, this downfield shift is about 30 ppm; for carbon centered clusters, it is about 60 ppm. As shown in our calculation results (Table 1), the progression of bridging halide from Cl to I reduces the $t_{1u}^* - t_{1u}$ gap by about 0.60 and 0.64 eV for boron- and carbon-centered clusters, respectively. The change of bridging halides is accompanied with structural changes. For example, as the bridging halides progresses from Cl to I, the Zr−B distance increases by 0.07 Å and the Zr−C distance increases by 0.05 Å, from which we infer a weakening of the Zr-interstitial bonding and a decrease the $t_{1u}^* - t_{1u}$ gap. Additional calculations on compressed $[(Zr_6BI_{12})(H_2O)]^+$ and expanded $[(Zr_6BCl_{12})(H_2O)]^+$ clusters (core sizes of both clusters being the same as that of the bromide supported cluster) show that the change in core size accounts for only about 12% (I) and 50% (Cl) of the change in the $t_{1u}^* - t_{1u}$ energy gap. The greater part of the change in the $t_{1u}^* - t_{1u}$ energy gap derives

from the change in the electronegativity of bridging halides. The greater electronegativity of the lighter halides withdraws more charge from the zirconium atoms, thereby lowering the energy of the Zr 4d orbitals. This leads to an increase in the t_{1u}*−t_{1u} energy gap because the bonding orbital is more localized on the Zr atoms and t_{1u}* orbital is more localized on the B atom, which accounts for most of the change we calculate. In reality, of course, the influences of the halide electronegativity and cluster core size are not entirely separable.

The chemical shifts of interstitial atoms are sensitive to the binding of terminal ligands.[1,2] The terminal ligands exert a subtler effect on chemical shift differences than the bridging ligands. Nevertheless, as seen from Figure 6, the trend of ^{11}B chemical shift with respect to terminal ligand change can also be roughly correlated with the t_{1u}*−t_{1u} gap. We found that the change of the ^{11}B chemical shift is in accordance with the binding strength of neutral ligands established in competition experiments, which decreases in the order of OPR_3 > CH_3OH > PR_3 > $NCCH_3$.[2] According to our calculations, coordination to stronger σ donors tends to increase the t_{1u}*−t_{1u} gap, and therefore causes the ^{11}B nucleus to be more shielded. However, a series of four calculations in which we changed Zr−O bond length of $[(Zr_6BCl_{12})(H_2O)_6]^+$ from 2.231 to 2.381 Å (the experimental Zr−O bond length is 2.281 Å) in 0.05 Å intervals suggests that more than a change in the t_{1u}*−t_{1u} gap is involved. Elongation of the Zr−O bonds leads to gradual (computed) deshielding of the interstitial boron by 2.7 ppm, but $\Delta E(t_{1u}$*−$t_{1u})$ decreases by only 0.005 eV. This suggests that rehybridization among the cage t_{1u} orbitals also occurs as the donor strength of terminal ligands varies. Overall, however, we can qualitatively correlate the trend of chemical shifts with the change in t_{1u}*−t_{1u} gap.

Calculations on the 16-CBE compound $Zr_6I_{12}C$ can be compared with the $[(Zr_6CX_{12})(H_2O)_6]^{2+}$ series. The t_{1u}*−t_{1u} gap for this 16 CBE system is 0.26 eV greater than that of $[(Zr_6CI_{12})(H_2O)_6]^{2+}$ (DMol^3 result). After taking into account of the systematic difference between DMol^3 and ADF, the t_{1u}*−t_{1u} energy gap for $Zr_6I_{12}C$ is only slightly greater than that of $[(Zr_6CI_{12})(H_2O)_6]^{2+}$. Figure 7 shows it to fall in the expected position in the correlation of chemical shift with $\Delta E^{-1}(t_{1u}$*−$t_{1u})$. It is interesting that $Zr_6I_{12}C$ fits reasonably well into our correlative scheme, despite the fact that it is not isoelectronic; there are two extra electrons that fill what was the a_{2u} symmetry LUMO of the 14 CBE clusters. As we have indicated, however, the a_{2u} orbital is of the wrong symmetry to exert any influence on the chemical shift.

Quantitative Analyses. *Basis Set Effects.* For quantitative evaluation of the chemical shielding properties, we studied the basis set effect on nonrelativistic chemical shieldings with the model compound $[(Zr_6BCl_{12})(H_2O)_6]^+$. We used the TZP basis set with polarization functions for zirconium, to help ensure a proper description of the metal−metal bonding. Both TZP and TZ2P basis sets were tried for interstitial boron, and for chlorine and oxygen ligand atoms DZP and TZP basis sets were varied. Basis sets of the same quality as oxygen were used for hydrogen. We found that although the change of basis sets generally causes little change (less than 0.5 ppm) in the total isotropic shielding constant, it does in some cases have larger effect on partitioning of the shielding between the diamagnetic and paramagnetic terms. The extra *f* polarization function involved in the TZP → TZ2P basis set change for boron has a negligible effect on both paramagnetic and diamagnetic shielding constants. The shielding constants are only slightly sensitive to the basis set change of oxygen and hydrogen, but are more sensitive to the chlorine basis set (12 ppm change) where changes in the paramagnetic and diamagnetic shieldings offset and the net change in the total shielding is small. In our calculations, we used the larger basis set.

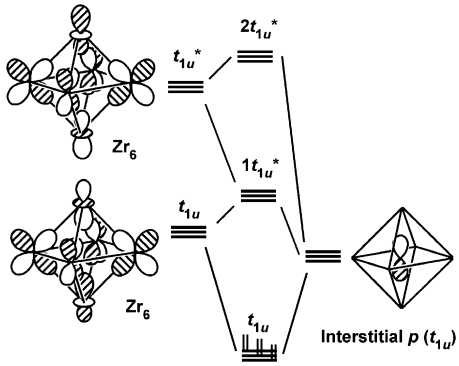

Figure 8. Schematic representation of interactions between interstitial 2p orbitals and two sets of zirconium cage orbitals with t_{1u} symmetry.

The Diamagnetic Term (σ_d) and the Paramagnetic Term (σ_p). Absolute chemical shielding properties were calculated and expressed in terms of diamagnetic and paramagnetic contributions according to the formulation of Schreckenbach, Ziegler, and their co-workers.[25,28] Within the group of boron-centered clusters, the calculated diamagnetic terms (σ_d) are fairly constant with variation of terminal ligands and bridging halides, except for $[(Zr_6BI_{12})(H_2O)_6]^+$ and $[(Zr_6BCl_{12})(OPH_3)_6]^+$, for which the σ_d terms are 20 and 10 ppm greater, respectively. Of the carbon-centered clusters, an appreciable increase (maximum 21 ppm) from the rest of the series was found in the diamagnetic shielding of $[(Zr_6CI_{12})(H_2O)_6]^{2+}$. For boron-centered clusters, the calculated paramagnetic shielding terms alone correlate somewhat better with measured chemical shifts than with total calculated shifts as suggested by Figure 4. There are fewer homoleptic cluster complexes available for experimental comparison in the case of carbon-centered clusters, but the systems we do have available show the dominant role of the paramagnetic term (Figure 5).

Contribution to the Paramagnetic Term from Other Virtual MOs. The output of the ADF-EPR/NMR program gives a detailed orbital-by-orbital analysis to both diamagnetic and paramagnetic terms. The paramagnetic term is further broken down to the occupied-occupied term (oc-oc), the occupied-virtual term (oc-vir), the gauge invariance term, and the frozen core term (b1).[28,60] Both gauge-invariance and frozen core terms are small. The absolute values of the oc-oc terms are less than 40 ppm for all clusters calculated. For the boron-centered and carbon-centered clusters, the oc-oc terms are respectively 5−10% and 1−5% of the magnitude of the oc-vir terms; as expected then, the oc-vir term gives the predominant contribution to the paramagnetic shielding. A closer examination of the orbital analysis of the oc-vir term is therefore in order. The orbital analysis shows that for most carbon and boron centered clusters, at least two sets of virtual orbitals within t_{1u} manifold couple with the occupied t_{1u} orbitals. Even though the two sets of t_{1u}* orbitals are approximately 3 eV apart in energy, the magnitude of their contributions to the paramagnetic term are comparable. Modification has been made to the original picture of molecular bonding based on the contours of the t_{1u}* orbitals (Figure 8). As seen in Figure 8, the t_{1u}* orbitals contributing to the chemical shielding are bonding combinations of the interstitial 2p orbitals with not only the bonding zirconium cage orbitals but also the antibonding zirconium cage orbitals with t_{1u} symmetry. For the $[(Zr_6BCl_{12})(NCH)_6]^+$ with rigorous O_h

symmetry, the π^* orbital from NCH is both within the energy range and of the right symmetry to interact with the $1t_{1u}^*$ to split it further into two sets. This complication is probably the source of greater deviation for the NCH-bound cluster is within the series in the chemical shift−energy gap correlation (Figure 6). As most model compounds we studied exhibit D_{3d} symmetry, the contours of orbitals of interest are more complicated than can be derived from simple combination of MOs shown in Figures 2 and 8. Nevertheless, it is quite clear that the pseudo-$1t_{1u}^*$ orbitals exhibit bonding interactions between the interstitial and the basal zirconium atoms and π antibonding interaction with the axial zirconium; the $2t_{1u}^*$ orbital exhibits only antibonding interactions. Mixing from the antibonding zirconium cage orbitals is important for chemical shielding as it stabilizes the virtual t_{1u} orbitals by introducing some bonding interaction between the interstitial p and the zirconium cage orbitals. For the $[(Zr_6CX_{12})(H_2O)_6]^{2+}$ series, coupling from an e_u^* set to the t_{1u} orbitals was also seen. This e_u^* set is so close in energy to the $1t_{1u}^*$ orbitals that within the actual D_{3d} symmetry of the computed cluster, it acquires small amount of interstitial 2p character.

Conclusions

In this DFT study, we have established the approximate inverse proportionality between the interstitial chemical shift and the energy gap $\Delta E(t_{1u}^*-t_{1u})$ for boron- and carbon-centered zirconium halide clusters. For a given interstitial atom, there is therefore a qualitative correlation between the strength of cage-interstitial bonding and the shielding of the interstitial nucleus. On a quantitative level, the DFT/GIAO method successfully reproduces trends in the ^{11}B and ^{13}C chemical shifts. The maximum relative errors for the calculated ^{11}B and ^{13}C isotropic chemical shifts are 8% and 12% respectively. A detailed orbital−orbital analysis confirms that paramagnetic contributions are indeed dominated by interaction between Zr_6 cage orbitals of t_{1u} symmetry and the 2p orbitals of the interstitial atom, though the simple two-orbital model that focuses on a single $t_{1u}^*-t_{1u}$ energy oversimplifies to some extent. Thus, the correlation of interstitial chemical shift with the energy gap $\Delta E(t_{1u}^*-t_{1u})$ is qualitatively useful but neglects some significant quantitative variation in the diamagnetic contributions and the matrix elements coupling occupied and virtual orbitals. Nevertheless, it is found for both B- and C-centered clusters, the correlation between the calculated and experimental chemical shifts is quite comparable to that between the measured chemical shifts and the energy gaps.

Acknowledgment. We thank Lindsay Roy for help with calculations and Xiaobing Xie for many of his unpublished measurements. We thank the Robert A. Welch Foundation for its support through Grant A-1132, the National Science Foundation for its support through Grant CHE-9623255. We also thank the Supercomputing Facility and Laboratory for Molecular Simulation at Texas A&M University for computing time and other support. The NSF is gratefully acknowledged for its support of the latter facility.

Supporting Information Available: Geometry specification of cluster model compounds, derivation of energy gap between the t_{1u} and the hypothetical t_{1u}^* orbitals of Zr_6CI_{12}, and comparison of energy gap $\Delta E(t_{1u}^*-t_{1u})$ of $[(Zr_6CX_{12})(H_2O)_6]^{2+}$ series calculated by use of DMol^3 and ADF programs. This material is available free of charge via the Internet at http://pubs.acs.org.

References and Notes

(1) Harris, J. D.; Hughbanks, T. *J. Am. Chem. Soc.* **1997**, *119*, 9449.
(2) Xie, X.; Reibenspies, J. H.; Hughbanks, T. *J. Am. Chem. Soc.* **1998**, *120*, 11391.
(3) Xie, X.; Hughbanks, T. *Inorg. Chem.* **2000**, *39*, 555.
(4) Xie, X.; Jones, J. N.; Hughbanks, T. *Inorg. Chem.* **2001**, *40*, 522.
(5) Xie, X.; Hughbanks, T. *Inorg. Chem.* **2002**, *41*, 1824.
(6) Hong, F. E.; Coffy, T. J.; McCarthy, D. A.; Shore, S. G. *Inorg. Chem.* **1989**, *28*, 3284.
(7) Housecroft, C. E.; Matthews, D. M.; Waller, A.; Edwards, A. J.; Rheingold, A. L. *J. Chem. Soc., Dalton Trans.* **1993**, 3059.
(8) Khattar, R.; Puga, J.; Fehlner, T. P.; Rheingold, A. L. *J. Am. Chem. Soc.* **1989**, *111*, 1877.
(9) Bordoni, S.; Heaton, B. T.; Seregni, C.; Strona, L.; Goodfellow, R. J.; Hursthouse, M. B.; Thornton-Pett, M.; Martinengo, S. *J. Chem. Soc., Dalton Trans.* **1988**, 2103.
(10) Bradley, J. S. *Philos. Trans. R. Soc. London, Ser. A* **1982**, *308*, 103.
(11) Pergola, R. D.; Bandini, C.; Demartin, F.; Diana, E.; Garlaschelli, L.; Stanghellini, P. L.; Zanello, P. *J. Chem. Soc., Dalton Trans.* **1996**, 747.
(12) Della Pergola, R.; Cinquantini, A.; Diana, E.; Garlaschelli, L.; Laschi, F.; Luzzini, P.; Manassero, M.; Repossi, A.; Sansoni, M.; Luigi Stanghellini, P.; Zanello, P. *Inorg. Chem.* **1997**, *36*, 3761.
(13) Blohm, M. L.; Gladfelter, W. L. *Organometallics* **1985**, *4*, 45.
(14) Mason, J. *J. Am. Chem. Soc.* **1991**, *113*, 24.
(15) Fehlner, T. P.; Czech, P. T.; Fenske, R. F. *Inorg. Chem.* **1990**, *29*, 3103.
(16) Duer, M. J.; Wales, D. J. *Polyhedron* **1991**, *10*, 1749.
(17) Kaupp, M. *Chem. Commun.* **1996**, 1141.
(18) Khattar, R.; Fehlner, T. P.; Czech, P. T. *New J. Chem.* **1991**, *15*, 705.
(19) Ziegler, T. *Chem. Rev.* **1991**, *91*, 651.
(20) Noodleman, L.; Peng, C. Y.; Case, D. A.; Mouesca, J. M. *Coord. Chem. Rev.* **1995**, *144*, 199.
(21) Siegbahn, P. E. M.; Blomberg, M. R. A. *Chem. Rev.* **2000**, *100*, 421.
(22) Buhl, M.; Kaupp, M.; Malkina, O. L.; Malkin, V. G. *J. Comput. Chem.* **1999**, *20*, 91.
(23) Cheeseman, J. R.; Trucks, G. W.; Keith, T. A.; Frisch, M. J. *J. Chem. Phys.* **1996**, *104*, 5497.
(24) Rauhut, G.; Puyear, S.; Wolinski, K.; Pulay, P. *J. Phys. Chem.* **1996**, *100*, 6310.
(25) Schreckenbach, G.; Ziegler, T. *J. Phys. Chem.* **1995**, *99*, 606.
(26) Schreckenbach, G.; Ziegler, T. *Theor. Chem. Acc.* **1998**, *99*, 71.
(27) Ruiz-Morales, Y.; Schreckenbach, G.; Ziegler, T. *J. Phys. Chem.* **1996**, *100*, 3359.
(28) Bouten, R.; Baerends, E. J.; van Lenthe, E.; Visscher, L.; Schreckenbach, G.; Ziegler, T. *J. Phys. Chem. A* **2000**, *104*, 5600.
(29) Wolff, S. K.; Ziegler, T. *J. Chem. Phys.* **1998**, *109*, 895.
(30) Bagno, A.; Saielli, G. *Chem. Eur. J.* **2003**, *9*, 1486.
(31) Buhl, M.; Hamprecht, F. A. *J. Comput. Chem.* **1998**, *19*, 113.
(32) Xu, X. P.; Au−Yeung, S. C. F. *J. Am. Chem. Soc.* **2000**, *122*, 6468.
(33) Tian, Y.; Hughbanks, T. *Inorg. Chem.* **1995**, *34*, 6250.
(34) Sun, D.; Hughbanks, T. *Inorg. Chem.* **1999**, *38*, 992.
(35) Xie, X.; Hughbanks, T. *Angew. Chem., Int. Ed. Engl.* **1999**, *38*, 1777.
(36) ADF2002.02. SCM, Theoretical Chemistry, Vrije Universiteit, Amsterdam, The Netherlands.
(37) Guerra, C. F.; Snijders, J. G.; Te Velde, G.; Baerends, E. J. *Theor. Chem. Acc.* **1998**, *99*, 391.
(38) Te Velde, G.; Bickelhaupt, F. M.; Baerends, E. J.; Fonseca Guerra, C.; Van Gisbergen, S. J. A.; Snijders, J. G.; Ziegler, T. *J. Comput. Chem.* **2001**, *22*, 931.
(39) Becke, A. D. *Phys. Rev. A: At., Mol., Opt. Phys.* **1988**, *38*, 3098.
(40) Lee, C.; Yang, W.; Parr, R. G. *Phys. Rev. B: Condens. Matter* **1988**, *37*, 785.
(41) Schreckenbach, G.; Ziegler, T. *Int. J. Quantum Chem.* **1996**, *60*, 753.
(42) Wolff, S. K.; Ziegler, T.; van Lenthe, E.; Baerends, E. J. *J. Chem. Phys.* **1999**, *110*, 7689.
(43) We thank Scientific Computing & Modeling NV for uncovering this source of error in calculations using symmetry.
(44) Xie, X.; Hughbanks, T. *Solid State Sci.* **1999**, *1*, 463.
(45) Xie, X.; Hughbanks, T., unpublished results.
(46) Shen, J.; Hughbanks, T. unpublished results.
(47) Chen, L.; Cotton, F. A. *Inorg. Chim. Acta* **1997**, *257*, 105.
(48) Atoji, M.; Lipscomb, W. N. *J. Chem. Phys.* **1957**, *27*, 195.
(49) Levy, H. A.; Brockway, L. O. *J. Am. Chem. Soc.* **1937**, *59*, 2085.
(50) Brockway, L. O.; Jenkins, H. O. *J. Am. Chem. Soc.* **1936**, *58*, 2036.
(51) Sheehan, W. F., Jr.; Schomaker, V. *J. Am. Chem. Soc.* **1952**, *74*, 3956.
(52) Smith, J. D.; Corbett, J. D. *J. Am. Chem. Soc.* **1985**, *107*, 5704.

(53) Delley, B. *J. Chem. Phys.* **2000**, *113*, 7756.
(54) Delley, B. *Comput. Mater. Sci.* **2000**, *17*, 122.
(55) Carrington, A.; McLachlan, A. D. *Introduction to Magnetic Resonance*; Chapman and Hall: London, 1979.
(56) Onak, T. P.; Landesman, H.; Williams, R. E.; Shapiro, I. *J. Phys. Chem.* **1959**, *63*, 1533.
(57) Kaupp, M.; Malkina, O. L.; Malkin, V. G.; Pyykko, P. *Chem.-Eur. J.* **1998**, *4*, 118.
(58) Abragam, A.; Bleaney, B. *Electron Paramagnetic Resonance of Transition Ions*; Dover: New York, 1986.
(59) NIST Atomic Spectra Database: http://physics.nist.gov/cgi-bin/AtData/main_asd
(60) In magnetic computations, there is an unphysical dependence on the gauge origin for the magnetic vector potential when a finite basis set is used; the "gauge-invariance term" is part of the elimination of this artifact in the GIAO approach. See reference 28 for details.